RSC Advances

PAPER

View Article Online
View Journal | View Issue

Cite this: *RSC Adv.*, 2017, **7**, 46644

Nano-Fe_3O_4@SiO_2-supported boron sulfonic acid as a novel magnetically heterogeneous catalyst for the synthesis of pyrano coumarins†

Mahnaz Farahi,* Bahador Karami, Raziyeh Keshavarz and Foroogh Khosravian

Received 26th July 2017
Accepted 20th September 2017

DOI: 10.1039/c7ra08253c

rsc.li/rsc-advances

In this study, a novel magnetically heterogeneous catalyst based on the immobilization of boron sulfonic acid onto Fe_3O_4@SiO_2 nanoparticles (Fe_3O_4@SiO_2–BSA) is reported. Fe_3O_4@SiO_2–BSA was characterized *via* FT-IR, X-ray diffraction patterns (XRD), scanning electron microscopy (SEM), energy-dispersive X-ray spectroscopy (EDS), and vibrating sample magnetometer (VSM) analysis. The performance ability of this catalyst including acid sites was evaluated for the synthesis of pyrano coumarins under solvent-free conditions with high yields. Thermal stability of the catalyst and its easy separation by a magnetic field make this catalyst a good heterogeneous system and a useful alternative to other heterogeneous catalysts.

Introduction

Supported heterogeneous catalysts as environmentally friendly materials play a pivotal role in modern science and technology, in particular, in the organic synthesis area.[1–3] Because of the many advantages of catalyst immobilization on solid supports, including easy handling, low solubility, increasing selectivity of the reactions, and non-toxicity, it is a technique that is widely used.[4] Nanostructure supports are also advantageous because they exhibit higher activity and selectivity than their corresponding bulk materials.[5–8] As the diameter of the particle decreases to the nanometer scale, the external surface area becomes available for chemical transformations.[9] Recent studies show that magnetite (Fe_3O_4) nanoparticles have unique properties such as simple isolation from the reaction mixture using an external magnetic field, high surface area, thermal stability, low cost, their potential to immobilize functional groups, and excellent recyclability, which make them useful supports to prepare reusable heterogenous catalysts.[10–12] A protective shell of silica as a coating can be formed on the surface of Fe_3O_4 nanoparticles to prevent them from oxidizing in an air atmosphere, provide simple surface functionalization, and enable aggregation between particles.[13,14]

Boron sulfonic acid, as a solid acid catalyst that was first introduced by Kiasat *et al.*, and silica boron sulfonic acid have many advantages such as simplicity in preparation, availability of precursor, economically benign, non-toxicity, and high activity/selectivity with excellent yields in various chemical processes.[15]

Synthesis of hybrid heterocycles that contain biologically active skeletons is an interesting subject in organic synthesis.[16,17] The chromene ring system is used regularly as a scaffold in medicinal and agricultural chemistry.[18,19] Pyrano coumarins as a fused dihydropyran with a chromene nucleus received great attention due to their wide range of applications in various fields of chemistry.[20,21] They have exhibited various pharmacological activities such as anti-HIV, antitumor, anticancer, antibacterial, and anti-inflammatory properties.[22,23] Moreover, they can also be employed as cosmetics and pigments and utilized as potential biodegradable agrochemicals.[24,25] The unique properties and broad applications of pyrano coumarins have promoted extensive studies for the synthesis of these useful compounds.

Because one-pot multi-component reactions (MCRs) play an important role in combinatorial chemistry, this field remained one of the most interesting areas of research in recent years. During multi-component reactions, target compounds are formed by joining at least three functional groups through covalent bonds.[26] These reactions represent a very useful tool for the synthesis of complex molecules with potential biological properties because of their effective atom economy, convergent nature, and brief and straightforward experimental procedures.[27]

Herein, in continuation of our studies in the field of heterogeneous catalysts[28–31] and according to importance of pyrano coumarins, we wish to disclose, for the first time, the preparation and characterization of novel immobilized boron sulfonic acid onto Fe_3O_4@SiO_2 nanoparticles (Fe_3O_4@SiO_2–BSA) as well as the examination of their catalytic application in the synthesis of pyrano coumarin derivatives.

Experimental

All chemicals used in this research were purchased from Fluka and Merck chemical companies. The obtained products were identified by comparison of their spectral data and physical properties with previously reported data. The monitoring of the

Department of Chemistry, Yasouj University, Yasouj, Iran, 75918-74831. E-mail: farahimb@yu.ac.ir; Fax: +98-7412242167

† Electronic supplementary information (ESI) available. See DOI: 10.1039/c7ra08253c

reaction progress and determination of purity of the compounds were accomplished using TLC performed with silica gel SIL G/UV254 plates. Melting points were determined by an electrothermal KSB1N apparatus and are uncorrected. The NMR spectra of ^{1}H in DMSO were recorded on a Bruker Avance Ultra Shield 400 MHz spectrometer, and ^{13}C NMR spectra were recorded at 100 MHz using TMS as an internal standard. Infrared (IR) spectra were obtained with a JASCO Fourier transform-infrared (FT-IR)/680 spectrometer using KBr pellets. X-ray powder diffraction (XRD) patterns were recorded using a Bruker AXS (D8 Advance) X-ray diffractometer with Cu Kα radiation ($\lambda = 0.15418$ nm). The measurement was made in 2θ ranging from 10° to 80° at the speed of 0.05° min^{-1}. Energy dispersive spectroscopy (EDS) was performed using a TESCAN Vega model instrument. The morphology of the particles was observed by scanning electron microscopy (SEM) under an acceleration voltage of 26 kV. The magnetic measurement was carried out in a vibrating sample magnetometer (VSM; Kashan University, Kashan, Iran) at room temperature.

Preparation of Fe_3O_4

To synthesize Fe_3O_4 magnetic nanoparticles through a chemical coprecipitation method, a solution of $FeCl_3\cdot 6H_2O$ (2.7 g, 10 mmol) and $FeCl_2\cdot 4H_2O$ (1 g, 5 mmol) in 45 mL double distilled water was mechanically stirred under an argon atmosphere at 80 °C for 30 min. In the next step, a sodium hydroxide solution (5 mL, 10 M) was gradually added dropwise. After continuous stirring at 80 °C for 1 h under an argon atmosphere, the black precipitate of Fe_3O_4 magnetic nanoparticles was decanted using an external magnetic field. The product was washed with double distilled water until pH 9 was obtained and then dried at 60 °C under a vacuum.[32]

Procedure for the synthesis of Fe_3O_4-silica-coated nanoparticles

According to the current method in the literature, a suspension containing Fe_3O_4 magnetic nanoparticles (1 g) was sufficiently dispersed in a mixture of ethanol (80 mL), distilled water (20 mL), concentrated ammonia aqueous solution (3 mL, 28%), and tetraethyl orthosilicate (0.5 mL). The reaction mixture was heated under reflux for 12 h. The Fe_3O_4-silica-coated (Fe_3O_4@-SiO_2) was separated by a magnet, washed several times with ethanol, and dried at 60 °C in air.[33]

Procedure for Fe_3O_4@SiO_2–$OB(OH)_2$

A saturated solution of boric acid was added to a slurry containing Fe_3O_4@SiO_2 nanoparticles (8 g) in dry toluene (45 mL). The mixture was refluxed for 24 h. The resultant suspension was collected using an external magnet and washed several times with distilled water and then methanol. It was dried at 80 °C to obtain the brown solid named nano Fe_3O_4@SiO_2–$OB(OH)_2$.[34]

Procedure for the preparation of Fe_3O_4@SiO_2–$OB(OSO_3H)_2$

In the final stage, a 100 mL suction flask was equipped with a dropping funnel containing chlorosulfonic acid (7.64 g, 0.066 mol), dry chloroform (40 mL), one argon inlet, and a gas outlet tube for conducting HCl gas over an adsorbing solution (10% NaOH). Then, Fe_3O_4@SiO_2–$OB(OH)_2$ (7.5 g) was charged into the flask. Chlorosulfonic acid was added drop-wise over a period of 60 min at 0 °C. HCl gas immediately evolved from the reaction vessel. When the addition was completed, the mixture was sonicated for 1 h. The functionalized magnetic nanoparticles were collected by a magnet. The supernatant was decanted, and the nanoparticles were washed with dry chloroform (3 × 5 mL) and then dried in high vacuum overnight.

General procedure for the synthesis of pyrano coumarins 4 and 6

Fe_3O_4@SiO_2–BSA (0.005 g) was added to a mixture of malononitrile/ethyl cyanoacetate, aryl aldehyde, and 5,7-dihydroxy-4-substituted coumarin/4-hydroxycoumarin at 80 °C under solvent-free conditions. The reaction progress was monitored by TLC (*n*-hexane/EtOAc, 3 : 2). After completion of the reaction, boiling EtOAc (10 mL) was added, and the catalyst was separated by filtration. To further purify the product, the obtained powder was recrystallized from EtOH.

Compound 4e. FT-IR (KBr): ν_{max} 3477, 3423, 3315, 1702, 1681 cm^{-1}. ^{1}H NMR (DMSO-d_6, 400 MHz) $\delta = 10.88$ (s, 1H), 7.61 (s, 2H), 7.25–7.05 (m, 5H), 6.39 (s, 1H), 6.04 (s, 1H), 3.50 (s, 2H), 3.44 (s, 1H), 2.66 (s, 3H), 1.02–1.11 (m, 3H) ppm. ^{13}C NMR (DMSO-d_6, 100 MHz) $\delta = 168.47$, 168.18, 159.97, 159.92, 159.45, 158.12, 158.12, 158.05, 154.23, 153.41, 147.54, 143.85, 143.69, 132.54, 131.78, 111.30, 110.01, 101.57, 98.09, 56.06, 24.11, 18.56, 14.27 ppm. Anal. calcd for $C_{22}H_{18}ClNO_6$: C, 61.76; H, 4.24; N, 3.27. Found: C, 61.70; H, 4.26; N, 3.31. MS (*m*/*z*): 427 $[M]^+$.

Compound 4h. FT-IR (KBr): ν_{max} 3413, 3311, 1687, 1625 cm^{-1}. ^{1}H NMR (DMSO-d_6, 400 MHz) $\delta = 10.81$ (s, 1H), 7.58 (s, 2H), 7.22–7.84 (m, 7H), 6.36 (s, 1H), 6.11 (s, 1H), 5.87 (s, 1H), 2.74 (m, 5H), 1.06 (t, $J = 5.22$ Hz, 3H) ppm. ^{13}C NMR (DMSO-d_6, 100 MHz) $\delta = 168.41$, 160.07, 160.02, 159.44, 157.86, 153.89, 153.39, 147.61, 144.95, 132.86, 130.67, 127.87, 126.31, 126.23, 125.61, 125.16, 125.08, 124.93, 112.66, 111.32, 101.88, 98.08, 78.46, 50.23, 24.04, 18.52 ppm. Anal. calcd for $C_{26}H_{21}NO_6$: C, 70.42; H, 4.77; N, 3.16. Found: C, 70.38; H, 4.80; N, 3.21.

Compound 4r. FT-IR (KBr): ν_{max} 3402, 1728, 1663 cm^{-1}. ^{1}H NMR (DMSO-d_6, 400 MHz) $\delta = 11.10$ (s, 1H), 8.18 (d, $J = 8.8$ Hz, 2H), 7.44 (d, $J = 8.4$ Hz, 2H), 7.17 (s, 2H), 6.51 (s, 1H), 6.12 (s, 1H), 4.82 (s, 1H), 2.63 (s, 3H) ppm. ^{13}C NMR (DMSO-d_6, 100 MHz) $\delta = 160.02$, 159.76, 157.97, 155.17, 153.76, 153.10, 147.99, 146.72, 128.92, 124.29, 120.17, 112.12, 107.55, 102.46, 99.11, 56.64, 36.81, 24.49 ppm.

Compound 6c. FT-IR (KBr): ν_{max} 3380, 3311, 3189, 1714, 1675 cm^{-1}. ^{1}H NMR (DMSO-d_6, 400 MHz) $\delta = 7.92$ (d, $J = 8$ Hz, 1H), 7.82 (s, 1H), 7.80 (d, $J = 1.6$ Hz, 1H), 7.76 (d, $J = 1.6$ Hz, 1H), 7.74 (s, 1H), 7.72 (d, $J = 1.6$ Hz, 1H), 7.54 (s, 1H), 7.52 (s, 1H), 7.49 (t, $J = 3.6$ Hz, 2H), 7.47 (s, 1H) ppm. ^{13}C NMR (DMSO-d_6, 100 MHz) $\delta = 160.0$, 158.5, 154.4, 152.7, 149.2, 133.5, 132.9, 129.3, 125.1, 123.0, 119.4, 119.2, 117.0, 113.4, 110.4, 103.3, 57.3, 37.5 ppm. Anal. calcd for $C_{20}H_{11}N_3O_3$: C, 70.38; H, 3.25; N, 12.31. Found: C, 70.42; H, 3.20; N, 12.25.

Compound 6e. FT-IR (KBr): ν_{max} 3391, 3180, 1712, 1674, 1608 cm^{-1}. ^1H NMR (DMSO-d_6, 400 MHz) δ = 7.90 (dd, J = 8.0 Hz, 1H), 7.73–7.69 (m, 1H), 7.44–7.38 (m, 7H), 7.18 (d, J = 8.8 Hz, 2H), 6.95 (d, J = 8.8 Hz, 2H), 5.06 (s, 2H), 4.40 (s, 1H) ppm. ^{13}C NMR (DMSO-d_6, 100 MHz) δ = 159.51, 157.87, 157.45, 153.09, 152.06, 137.05, 135.60, 132.83, 128.76, 128.40, 127.79, 127.64, 124.63, 122.41, 119.30, 116.53, 114.61, 112.97, 104.19, 69.17, 58.09, 36.13 ppm.

Compound 6i. FT-IR (KBr): ν_{max} 3461, 3295, 3162, 1716, 1673, 1631 cm^{-1}. ^1H NMR (DMSO-d_6, 400 MHz) δ = 8.86 (s, 1H), 7.90 (d, J = 8 Hz, 1H), 7.74 (t, J = 8 Hz, 2H), 7.46–7.52 (m, 2H), 7.34 (s, 1H), 6.81 (d, J = 2 Hz, 1H), 6.72 (d, J = 2.1 Hz, 1H), 6.64 (d, J = 8.4 Hz, 1H), 4.35 (s, 1H), 3.94–4.01 (m, 2H), 1.32 (t, J = 6.8 Hz, 3H) ppm. ^{13}C NMR (DMSO-d_6, 100 MHz) δ = 160.0, 158.3, 153.4, 152.5, 146.5, 134.7, 133.2, 15.0, 122.9, 120.3, 119.8, 117.0, 116.0, 114.0, 113.5, 104.8, 64.4, 58.8, 36.9, 15.1 ppm. Anal. calcd for $C_{21}H_{16}N_2O_5$: C, 67.02; H, 4.28; N, 7.44. Found: C, 67.12; H, 4.20; N, 7.51.

Results and discussion

The new magnetic nano-catalyst Fe_3O_4@SiO_2–BSA was prepared following the protocol shown in Scheme 1. Firstly, in order to prepare the magnetic Fe_3O_4 nanoparticles, the chemical co-precipitation of Fe^{2+} and Fe^{3+} ions in NaOH solution was performed.[32] Subsequently, the silica-coated magnetic nanoparticles (Fe_3O_4@SiO_2) were easily achieved with the known Stober method.[32] Then, Fe_3O_4@SiO_2–$OB(OH)_2$ was synthesized from the reaction of Fe_3O_4@SiO_2 with boric acid in dry toluene under reflux.[34] Finally, the surface of Fe_3O_4@SiO_2–$OB(OH)_2$ was functionalized with chlorosulfonic acid to obtain Fe_3O_4@SiO_2–$OB(OSO_3H)_2$. Chemical analysis of prepared Fe_3O_4@SiO_2–$OB(OSO_3H)_2$ was performed using FT-IR, EDX, XRD, and SEM; magnetic measurements were performed using VSM.

The FT-IR spectra of Fe_3O_4, Fe_3O_4@SiO_2, Fe_3O_4@SiO_2@-$OB(OH)_2$, and Fe_3O_4@SiO_2–BSA were compared with each other (Fig. 1). The appearance of peaks around 570 cm^{-1}, 796 cm^{-1}, 1097 cm^{-1}, 478 cm^{-1}, and 3413 cm^{-1} in all of these four spectra are relevant to Fe–O stretching, Si–O–Si symmetric and asymmetric stretching, bending vibration, and OH vibration,

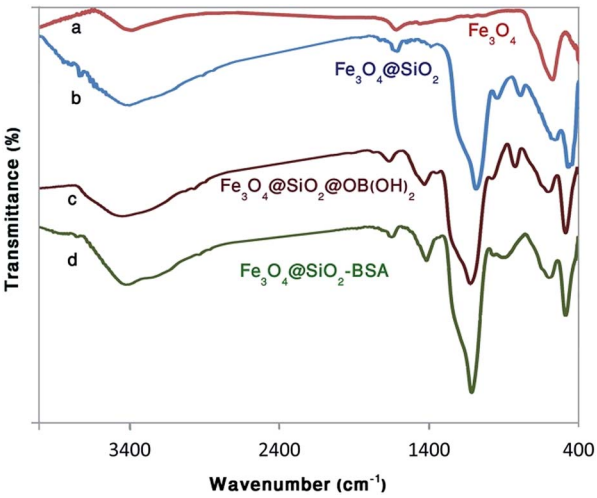

Fig. 1 The FT-IR of (a) Fe_3O_4, (b) Fe_3O_4@SiO_2, (c) Fe_3O_4@SiO_2@-$OB(OH)_2$, and (d) Fe_3O_4@SiO_2–BSA.

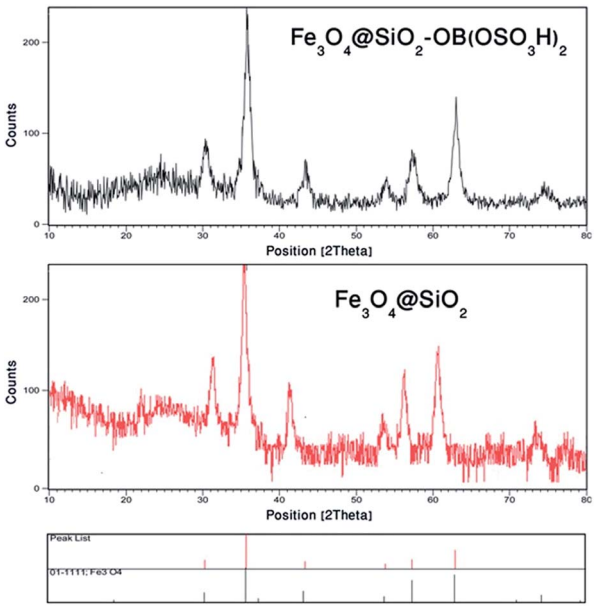

Fig. 2 XRD patterns of Fe_3O_4, Fe_3O_4@SiO_2, and Fe_3O_4@SiO_2–BSA.

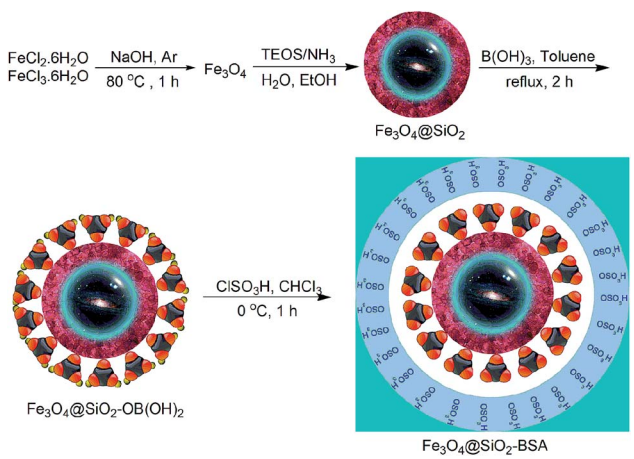

Scheme 1 Synthesis of Fe_3O_4@SiO_2–BSA.

respectively, which was confirmed to preserve the nano-structure of Fe_3O_4 and Fe_3O_4@SiO_2.[35] The peak in the region of approximately 1400 cm^{-1} of spectra c and d can be related to B–O.[36] The O=S=O asymmetric and symmetric stretching vibrations near 1200–1250 cm^{-1} and 1010–1100 cm^{-1}, and the S–O stretching vibration of $-SO_3H$ at 650 cm^{-1} and 3180 to 3419 cm^{-1} were seen in d spectra for the sulfonic group of the catalytic surface.[37]

To investigate the quantity of crystalline phases of the new catalyst, its XRD-diffraction pattern was obtained, as shown in Fig. 2. The control of six characteristic peaks at 30.3909, 35.7981, 43.4418, 53.9044, 57.4051, and 63.0226 that correspond to the (2 2 0), (3 1 1), (4 0 0), (4 2 2), (5 1 1), and (4 4 0) crystal planes is very important because the preservation of the cubic spinel structure could be strictly confirmed (JCPD 00-001-1111 standard). Additionally, there was a broad peak from 2θ = 19 to 28 that

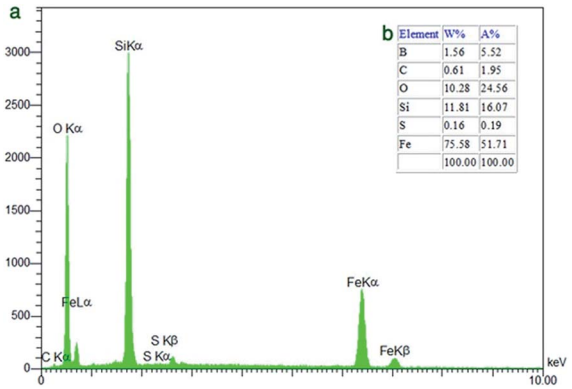

Fig. 3 (a) Energy-dispersive X-ray spectroscopy (EDS) spectra of Fe_3O_4@SiO_2–BSA. (b) EDS data for Fe_3O_4@SiO_2–BSA.

was due to the SiO_2 shells of the coated Fe_3O_4.[38] The other existing groups in the catalyst did not exhibit any changes in the crystal structure. The particle size of the prepared catalyst can be calculated using the Debye–Scherrer equation:

$$D = 0.94\lambda/\beta \cos\theta$$

where D is the average particle diameter, 0.94 is the Scherrer's constant, λ is the X-ray wavelength (1.5406 °A for Cu Kα), β is the half width of XRD diffraction lines, and θ is the Bragg's angle in degrees. The particle size relevant to the Debye–Scherrer equation is calculated as 88.8 nm.

Energy-dispersive X-ray spectroscopy (EDS) is one of the best approaches to determine catalyst purity. Fig. 3 shows the EDS spectra indicating the elemental composition of the catalyst. It contains no impurity elements other than Fe, O, Si, S, and B. It must be noted that failure of the boron peak is observed because of the overlap between peaks of boron and other elements.[36]

The SEM image of Fe_3O_4@SiO_2–BSA in Fig. 4 shows that the average diameter range was 58–86 nm, indicating good harmony in comparision with the calculated result from the Debye–Scherrer equation. Also, the uniform core–shell morphology was consistent

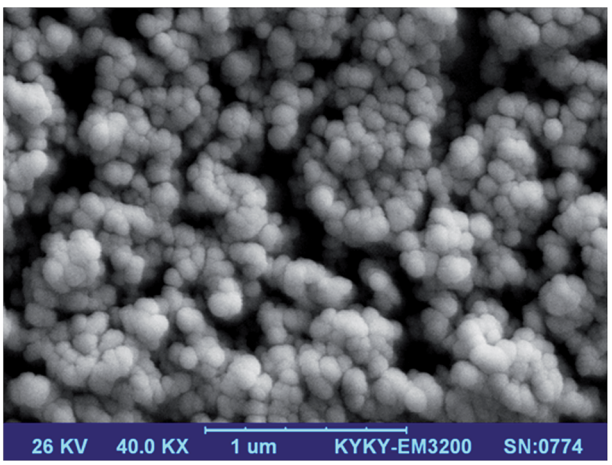

Fig. 4 SEM image of the catalyst.

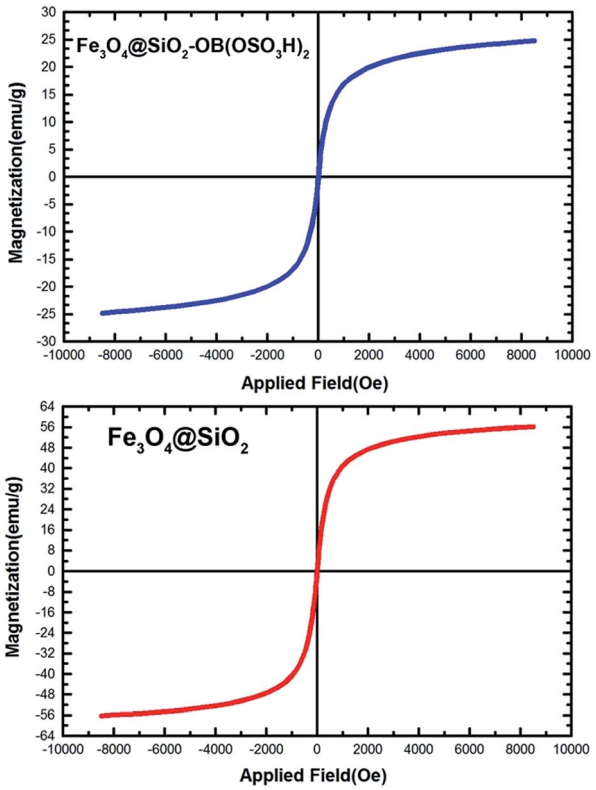

Fig. 5 The vibrating sample magnetometer (VSM) magnetization curves of Fe_3O_4@SiO_2–BSA in comparison with Fe_3O_4@SiO_2.

with the spherical shape of the Fe_3O_4 nanoparticles. We commonly used a vibrating sample magnetometer to evaluate the magnetic measurement of our catalyst. Fig. 5 shows the magnetic behavior at room temperature for the catalyst. The below magnetization curves indicate the saturation magnetization of Fe_3O_4@SiO_2 nanoparticles and Fe_3O_4@SiO_2–BSA, which were diminished to 24.8 emu g^{-1} from 56.2 emu g^{-1} for Fe_3O_4@SiO_2.

To show the catalytic activity of Fe_3O_4@SiO_2–BSA, it was used as a catalyst in the synthesis of a range of known and novel pyrano coumarins **4** and **6** *via* the three-component reactions of aryl aldehydes **1**, active methylene compound **2** (malononitrile or ethyl cyanoacetate), and hydroxycoumarin (5,7-dihydroxy-4-substituted coumarins **3** or 4-hydroxycoumarin **5**) under solvent-free conditions (Scheme 2).

To initiate the synthetic work, several 5,7-dihydroxy-4-substituted coumarins **3** were prepared in good yields according to previously published methods.[39] Subsequently, in order to find the most appropriate reaction conditions, a three-component reaction of ethyl cyanoacetate, benzaldehyde, and 4-methyl-5,7-dihydroxycoumarin was screened as a model reaction. The desired product was not produced in the absence of a catalyst even after a long reaction time. Therefore, the model reaction was performed using Fe_3O_4@SiO_2@$(CH_2)_3$-$OMoO_3H$ at various conditions. On the basis of the results obtained, we found that this reaction was efficiently performed in the presence of 0.005 g of Fe_3O_4@SiO_2–BSA at 80 °C under solvent-free conditions (Table 1).

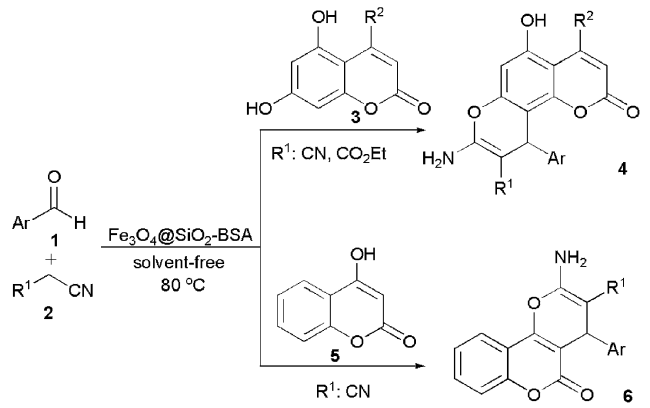

Scheme 2 Preparation of pyrano coumarins **4** and **6** in the presence of Fe_3O_4@SiO_2–BSA as catalyst.

Table 1 Screening conditions for the model reaction

Entry	Catalyst (g)	Solvent	T (°C)	Yield[a] (%)
1	0.001	None	70	30
2	0.002	None	70	40
3	0.003	None	70	45
4	0.004	None	70	47
5	0.005	None	70	70
6	0.006	None	50	70
7	0.005	None	60	60
8	0.005	None	80	90
9	0.005	None	90	90
10	0.005	None	100	90
11	0.005	MeOH	Reflux	65
12	0.005	EtOH	Reflux	67
13	0.005	EtOH/H_2O	Reflux	55
14	0.005	CH_3CN	Reflux	73
16	0.005	Toluene	Reflux	60

[a] Isolated yields.

With optimal conditions established, we then examined the scope of the reaction for the construction of various substrates including malononitrile, various aromatic aldehydes, and diverse 5,7-dihydroxy-4-substituted coumarin derivatives; the results are summarized in Table 2. In general, the reaction proceeded smoothly to afford the desired products **4** in good to excellent yields.

Encouraged by these results, we extended the catalytic activity of Fe_3O_4@SiO_2–BSA to condensation reactions of aromatic aldehydes, malononitrile, and 4-hydroxycoumarin to afford pyrano coumarins **6** (Scheme 2). A series of product **6** with different substituents was prepared from different aromatic aldehydes bearing electron-withdrawing and electron-donating groups (Table 3).

The structures of the obtained products **4** and **6** were deduced from their elemental analysis, IR, ^{1}H, and ^{13}C NMR spectroscopy and they were compared with authentic samples.[40–42] Although both electron-rich and electron-poor aldehydes afforded the desired products **4** and **6**, aldehydes having electron-withdrawing groups in comparison with those having electron-donating ones performed this transformation in better yields. This may be explained according to more positive charges located on the carbonyl group of aldehydes in electron-poor cases, which makes it a more reactive electrophile center.

Table 2 Fe_3O_4@SiO_2–BSA-catalyzed synthesis of pyrano coumarins **4**

Entry	Ar	R^1	R^2	Mp (°C)	Yield[a] (%)
4a	C_6H_5	CO_2Et	CH_3	260–262	90
4b	4-$CH_3C_6H_4$	CO_2Et	CH_3	280–282	75
4c	4-BrC_6H_4	CO_2Et	CH_3	215–217	86
4d	3-BrC_6H_4	CO_2Et	CH_3	271–273	90
4e	2-ClC_6H_4	CO_2Et	CH_3	274–276	93
4f	2,4-$Cl_2C_6H_3$	CO_2Et	CH_3	251–253	89
4g	2-Cl6-FC_6H_3	CO_2Et	CH_3	234–235	87
4h	1-Naphthyl	CO_2Et	CH_3	208–210	75
4i	C_6H_5	CN	CH_3	250–251	85
4j	4-ClC_6H_4	CN	CH_3	245–247	93
4k	3-ClC_6H_4	CN	CH_3	202–204	96
4l	2-ClC_6H_4	CN	CH_3	325–326	90
4m	2,4-$Cl_2C_6H_3$	CN	CH_3	320–321	85
4n	4-$CH_3C_6H_4$	CN	CH_3	221–222	70
4o	4-$OCH_3C_6H_4$	CN	CH_3	260–262	65
4p	2-$OCH_3C_6H_4$	CN	CH_3	300–301	70
4q	3-BrC_6H_4	CN	CH_3	296–298	90
4r	4-$NO_2C_6H_4$	CN	CH_3	341–342	85
4s	3-$NO_2C_6H_4$	CN	CH_3	390–391	87
4t	2-ClC_6H_4	CN	Ph	241–242	85
4u	2-ClC_6H_4	CN	CH_2Cl	305–306	91

[a] Isolated yield.

A plausible mechanism for the synthesis of pyrano coumarins is outlined in Scheme 3. Initially, intermediate **7** is formed *via* the Knoevenagel condensation of the aldehyde and active methylene compound. For the formation of pyrano coumarin **4**, adduct **8** results from a Michael-type addition of C-8 of dihydroxycoumarin to compound **7**. Subsequently, cyclization of intermediate **8** gives pyrano coumarin **4**. 4-Hydroxycoumarin can also attack

Table 3 Synthesis of pyrano coumarins **6** using Fe_3O_4@SiO_2–BSA

Entry	Ar	Mp (°C)	Yield[a] (%)
6a	C_6H_5	261–263	85
6b	4-$CH_3C_6H_4$	255–257	90
6c	4-CNC_6H_4	252–254	83
6d	4-Iso-propylC_6H_4	240–242	87
6e	4-BenzyloxyC_6H_4	268–269	78
6f	3-BrC_6H_4	276–277	95
6g	2-Cl 6-FC_6H_3	293–295	80
6h	1-Naphthyl	260–261	86
6i	3-OEt 4-OHC_6H_3	244–245	75
6j	Thiophene-2-yl	265–266	80
6k	4-$OCH_3C_6H_4$	246–248	85
6l	4-$NO_2C_6H_4$	260–262	90
6m	4-ClC_6H_4	262–264	87
6n	3-$NO_2C_6H_4$	263–265	80
6o	2-ClC_6H_4	269–271	83
6p	2,4-$Cl_2C_6H_3$	259–260	80

[a] Isolated yield.

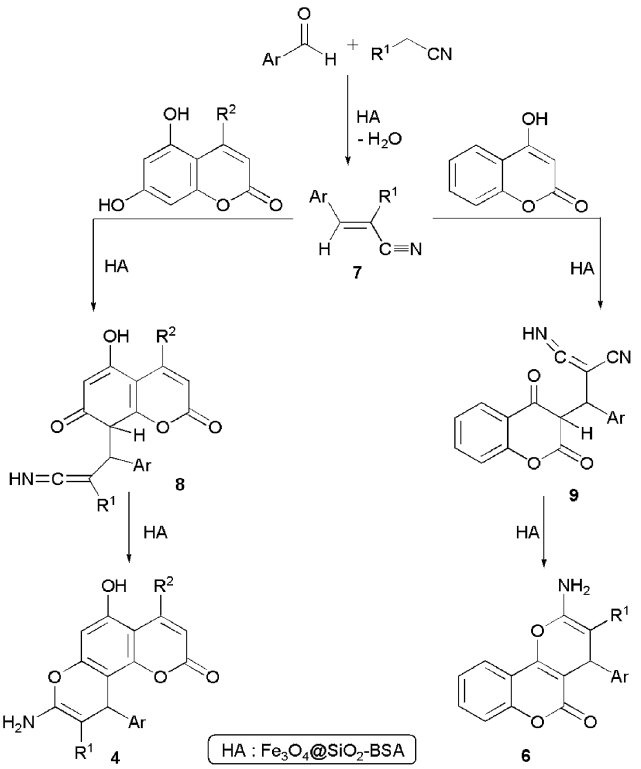

Scheme 3 Proposed mechanism for the synthesis of **4** and **6** in the presence of Fe_3O_4@SiO_2–BSA.

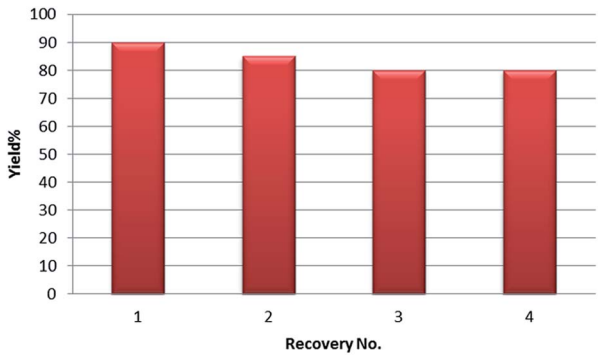

Fig. 6 Reusability study of Fe_3O_4@SiO_2–BSA in the synthesis of **4a** at 80 °C under solvent-free conditions.

intermediate **7** to produce **9,** which is then converted to pyrano coumarin **6** after an intramolecular cyclization.

The recovery and reusability of catalyst are quite preferable because they are eco-friendly procedures. The recovered Fe_3O_4@SiO_2–BSA from the model reaction for the synthesis of **4a** was regenerated by washing with chloroform and drying at 120 °C for 1 hour. Using the recycled catalyst four consecutive times in the model reaction gave the product with a gradually decreasing reaction yield (Fig. 6).

Conclusions

In summary, for the first time, a new modified magnetic nanoparticle-bearing boron sulfonic acid, Fe_3O_4@SiO_2–BSA, was prepared, characterized, and applied as a heterogeneous and efficient acid catalyst for the synthesis of a series of functionalized heterocyclic compounds containing the coumarin moiety *via* a one-pot three-component reaction. Our work presents a very simple reaction performed in the absence of hazardous organic solvents. Reusability of the catalyst, operational simplicity, and good chemical yields, combined with step- and atom-economic aspects, make this strategy highly attractive. It is worthwhile to note that the products are potentially valuable for further synthetic manipulation because of the presence of transformable functionalities.

Conflicts of interest

There are no conflicts to declare.

Acknowledgements

The authors gratefully acknowledge partial support of this work by Yasouj University, Yasouj, Iran.

Notes and references

1 J. E. Mondloch, E. Bayram and R. G. Finke, *J. Mol. Catal. A: Chem.*, 2012, **355**, 1.
2 P. Munnik, P. E. de Jongh and K. P. de Jong, *Chem. Rev.*, 2015, **115**, 6687.
3 J. A. Widegren and R. G. Finke, *J. Mol. Catal. A: Chem.*, 2003, **198**, 317.
4 J. M. Thomas and R. Raja, *Annu. Rev. Mater. Res.*, 2005, **35**, 315.
5 B. Levy, *J. Am. Chem. Soc.*, 1997, **119**, 12027.
6 M. B. Gawande, P. S. Branco and R. S. Varma, *Chem. Soc. Rev.*, 2013, **8**, 3175.
7 V. Polshettiwar and R. S. Varma, *Green Chem.*, 2010, **5**, 729.
8 M. Haruta, *Catal. Today*, 1997, **36**, 153.
9 E. A. Baranova, C. Bock, D. Ilin, D. Wang and B. MacDougall, *Surf. Sci.*, 2006, **600**, 3502.
10 J. Svoboda, *Magnetic methods for the treatment of minerals*, Elsevier, Amsterdam, New York, 1987.
11 H. Woo, K. Lee, S. Park and K. H. Park, *Molecules*, 2014, **19**, 699.
12 J. S. Yoo, *Catal. Today*, 1998, **44**, 27.
13 S. Villa, P. Riani, F. Locardi and F. Canepa, *Materials*, 2016, **9**, 826.
14 P. Riani, M. A. Lucchini, S. Thea, M. Alloisio, G. Bertoni and F. Canepa, *Inorg. Chem.*, 2014, **53**, 9166.
15 (*a*) A. R. Kiasat and M. Fallah-Mehrjardi, *J. Braz. Chem. Soc.*, 2008, **19**, 1595; (*b*) S. Sajjadifar, S. A. Mirshokraie, N. Javaherneshan and O. Louie, *Am. J. Org. Chem.*, 2012, **2**, 1.
16 B. N. Goswami, J. C. S. Kataky and J. N. Baruah, *J. Heterocycl. Chem.*, 1986, **23**, 1439.
17 Y. Yi, Y. Fu, P. Dong, W. Qin, Y. Liu, J. Liang and R. Shang, *Molecules*, 2017, **22**, 996.
18 N. Thomas and S. M. Zachariah, *Asian J. Pharm. Clin. Res.*, 2013, **6**, 11.

19 M. Costa, T. A. Dias, A. Brito and F. Proença, *Eur. J. Med. Chem.*, 2016, **10**, 487.
20 S. Pal, M. Khan, S. Karamthulla and L. Choudhury, *Tetrahedron Lett.*, 2015, **56**, 359.
21 S. Sheik Mansoor, K. Logaiya, K. Aswin and P. N. Sudhan, *J. Taibah Univ. Sci.*, 2015, **9**, 213.
22 A. M. M. El-Saghier, M. B. Naili, B. K. Rammash, N. A. Saleh and K. M. Kreddan, *ARKIVOC*, 2007, **xvi**, 83.
23 F. M. Abdelrazek, P. Metz, O. Kataeva, A. Jager and S. F. El-Mahrouky, *Arch. Pharm. Chem. Life Sci.*, 2007, **340**, 543.
24 F. M. Abdel-Galil, B. Y. Riad, S. M. Sherif and M. H. Elnagdi, *Chem. Lett.*, 1982, **11**, 1123.
25 I. H. El Azab, M. M. Youssef and M. A. Amin, *Molecules*, 2014, **19**, 19648.
26 B. H. Rotstein, S. Zaretsky, V. Rai and A. K. Yudin, *Chem. Rev.*, 2014, **114**, 8323.
27 M. Haji, *Beilstein J. Org. Chem.*, 2016, **12**, 1269.
28 M. Farahi, F. Tamaddon, B. Karami and S. Pasdar, *Tetrahedron Lett.*, 2015, **56**, 1887.
29 F. Tamaddon, M. Farahi and B. Karami, *J. Mol. Catal. A: Chem.*, 2011, **337**, 52.
30 M. Farahi, B. Karami, S. Alipour and L. T. Moghadam, *Acta Chim. Slov.*, 2014, **61**, 94.
31 M. Farahi, M. Davoodi and M. Tahmasebi, *Tetrahedron Lett.*, 2016, **57**, 1582.
32 M. C. Mascolo, Y. Pei and T. A. Ring, *Materials*, 2013, **6**, 5549.
33 W. Stober, A. Fink and E. Bohn, *J. Colloid Interface Sci.*, 1968, **26**, 62.
34 E. Yazdani, K. Azizi, A. Nakisa and A. Heydari, *J. Org. Chem. Res.*, 2015, **1**, 27.
35 A. Alizadeh, M. M. Khodaei, M. Beygzadeh, D. Kordestani and M. Feyzi, *Bull. Korean Chem. Soc.*, 2012, **33**, 2546.
36 X. Zhang, X. He, L. Chen and Y. Zhang, *J. Mater. Chem.*, 2012, **32**, 112.
37 A. Tadjarodi, R. Khodikar and H. Ghafuri, *RSC Adv.*, 2016, **6**, 63480.
38 G. Feng, D. Hub, L. Yang, Y. Cui, X. Cui and H. Li, *Sep. Purif. Technol.*, 2010, **74**, 253.
39 B. Karami and M. Kiani, *Catal. Commun.*, 2011, **14**, 62.
40 B. Karami, S. Khodabakhshi and K. Eskandari, *Tetrahedron Lett.*, 2012, **53**, 1445.
41 G. M. Ziarani, A. Badiei, M. Azizi and P. Zarabadi, *Iran. J. Chem. Chem. Eng.*, 2011, **30**, 59.
42 S. Khodabakhshi, B. Karami, K. Eskandari and S. J. Hoseini, *C. R. Chim.*, 2013, **17**, 35.